

Accepted Article

Title: Reversible pH responsive coacervate formation in lipid vesicles activates dormant enzymatic reactions

Authors: Celina Love, Jan Steinkühler, David T. Gonzales, Naresh Yandrapalli, Tom Robinson, Rumiana Dimova, and T.-Y. Dora Tang

This manuscript has been accepted after peer review and appears as an Accepted Article online prior to editing, proofing, and formal publication of the final Version of Record (VoR). This work is currently citable by using the Digital Object Identifier (DOI) given below. The VoR will be published online in Early View as soon as possible and may be different to this Accepted Article as a result of editing. Readers should obtain the VoR from the journal website shown below when it is published to ensure accuracy of information. The authors are responsible for the content of this Accepted Article.

To be cited as: *Angew. Chem. Int. Ed.* 10.1002/anie.201914893
Angew. Chem. 10.1002/ange.201914893

Link to VoR: <http://dx.doi.org/10.1002/anie.201914893>
<http://dx.doi.org/10.1002/ange.201914893>

RESEARCH ARTICLE

Reversible pH responsive coacervate formation in lipid vesicles activates dormant enzymatic reactions

Celina Love,^{[a] [b]} Jan Steinkühler,^[d] David T. Gonzales,^{[a] [b] [c]} Naresh Yandrapalli,^[d] Tom Robinson,^[d] Rumiana Dimova,^[d] T-Y Dora Tang*^{[a] [b]}

Abstract: *In situ*, reversible coacervate formation within lipid vesicles represents a key step in the development of responsive synthetic cellular models. Here we exploit the pH responsiveness of a polycation above and below its pKa, to drive liquid-liquid phase separation, to form single coacervate droplets within lipid vesicles. The process is completely reversible as coacervate droplets can be disassembled by increasing the pH above the pKa. We further show that pH triggered coacervation in the presence of low concentrations of enzymes activate dormant enzyme reactions by molecular up-concentration into the coacervate droplets. In conclusion, this work establishes a tuneable, pH responsive, enzymatically active multi-compartment synthetic cell. The system is readily transferred into microfluidics, making it a robust model for addressing general questions in biology such as the role of phase separation and its effect on enzymatic reactions using a bottom-up synthetic biology approach.

Introduction

Hybrid protocells with structural features of both membrane-bound and membrane-free compartmentalisation which respond to external stimuli, offer a blueprint for the genesis of dynamic synthetic cellular models. These provide distinct, unique and dynamic environments for the spatial organisation of reactions. Membrane-free coacervate microdroplets form via liquid-liquid phase separation between oppositely charged polypeptides, polynucleotides, polymers and macromolecules. This coacervation process has attracted a lot of attention as it has recently been demonstrated to be one of the driving forces of cellular condensate formation^{[1],[2],[3],[4]}. Cytoplasmic phase demixing^{[1],[2]} and synthetic liquid droplets^{[3],[4],[5]} have been shown to respond reversibly to changes in pH, salt, enzymes and light *in vivo* and *in vitro*. Here, regulation of the molecular charge or chemical structure of the coacervate forming components leads

to the mixing and de-mixing of the microdroplet resulting in dramatic changes in the local environment.

In addition, hybrid protocells of membrane-free sub-compartments within either water-in-oil (w/o) emulsions, giant vesicles^[6] or proteinosomes have been formed by spontaneous self-assembly methods in bulk or by using microfluidic methodologies^{[7],[8],[9]}. In these systems, changes in temperature or osmotic pressure from the exterior of the lipid vesicles have led to phase separation of aqueous two phase systems^{[10],[11]} and coacervates^[12] within the lipid vesicle. However, to the best of our knowledge there have been no examples of *in situ* formation of enzymatically active coacervates within lipid vesicles by an external pH stimulus.

To this end, we have developed a methodology for the *in situ*, pH reversible formation of coacervate microdroplets within giant unilamellar vesicles (GUVs). The membrane bounded lipid vesicle supports the isolation of the coacervate components from its exterior whilst permitting the transfer of water and protons across the lipid membrane^[13]. By exploiting the pH responsiveness of polylysine (PLys), a coacervate forming polypeptide^{[3],[14]}, we demonstrate that coacervate formation can be initiated within the lipid vesicle via an external change in pH. Above the pKa of PLys, coacervate formation with a counter polyanion is arrested and below the pKa of PLys, coacervate formation is triggered. We further show that this methodology is compatible with the encapsulation of enzymatic reactions and that *in situ* coacervate formation leads to the activation of enzymatic reactions by the up-concentration within a coacervate droplet. Our modular approach is robust, reproducible and can also be transferred to microfluidic methodologies, further demonstrating the versatility of the method.

It is not completely understood why membrane-free compartmentalisation is important in biological systems. It has been postulated that these dynamical liquid-liquid phase separation processes can play a role in regulating biochemical processes^{[15],[16],[17],[18]}. However, investigating these processes within the complex environment of the cell is challenging. Our work therefore offers key steps in the synthesis of dynamic protocellular systems in bottom-up synthetic biology and can be used to help test current models of the role of liquid-liquid phase

[a] C. Love, D. T. Gonzales, Dr. T-Y. D Tang*
Max Planck Institute of Molecular Cell Biology and Genetics
Pfotenhauerstraße 108, 01307 Dresden, Germany
*E-mail: tang@mpi-cbg.de

[b] C. Love, D. T. Gonzales, Dr. T-YD Tang*
Cluster of Excellence Physics of Life
TU Dresden, 01602 Dresden, Germany

[c] D. T. Gonzales
Center for Systems Biology Dresden, Pfotenhauerstraße 108,
01307 Dresden, Germany

[d] J. Steinkühler, N. Yandrapalli, R. Dimova, T. Robinson,
Max Planck Institute of Colloids and Interfaces
14424, Potsdam, Germany

Supporting information for this article is given via a link at the end of the document.

RESEARCH ARTICLE

separation in biology. Overall, this study presents a minimal model system for probing general phenomena in modern biology, where it is known that pH changes can lead to alterations of the

material properties of liquid-liquid phase separated droplets and affect biochemical enzymatic reactions inside cells.

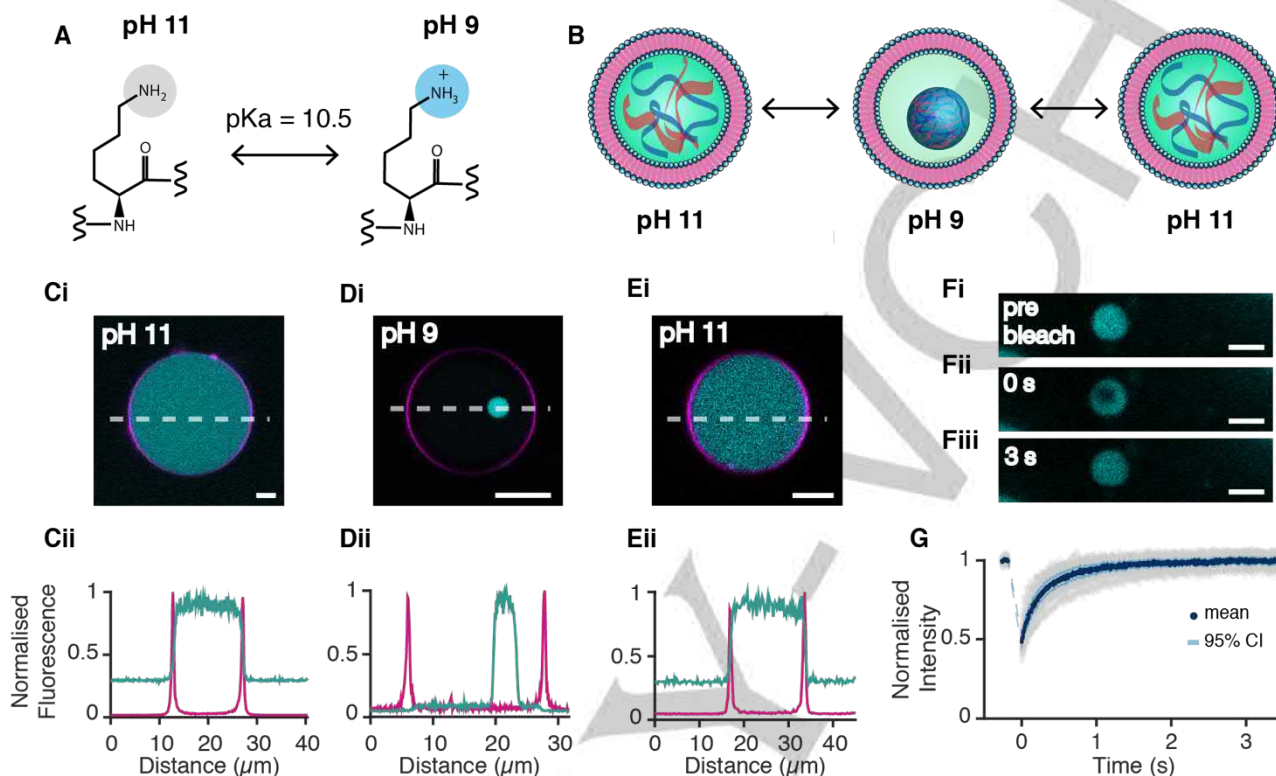


Figure 1. Reversible *in situ* formation of PLys/ATP coacervates in lipid vesicles by a reduction in pH. (A) Polylysine (PLys) switches between a cationic polymer to an uncharged polymer at its pKa of pH 10.5. (B) Cartoon depicting the pH-controlled formation of coacervate microdroplets within giant vesicles. (C-Ei) Fluorescent confocal images of GUVs made from POPC/Cholesterol containing PLys and ATP at a 4:1 molar ratio. Scale bar = 5 μm . (C) At pH 11, after washing the outer solution with iso-osmolar pH 11 buffer solution, (D) at pH 9, after the addition of iso-osmolar pH 7.3 buffer, (E) and after returning the pH to pH 11. (C-Eii) Corresponding intensity profiles (along the white dashed line) of confocal images of DiD fluorescence (magenta) and FITC-PLys fluorescence (cyan). Fluorescence intensities were normalized by the maximum intensity. (F) FRAP of coacervate microdroplets in lipid vesicles. Confocal fluorescence microscopy images of a PLys/ATP coacervate in a GUV before bleaching (i); at bleaching ($t=0$) (ii); and after recovery (3 s) (iii). Scale bar = 5 μm . (G) Corresponding FRAP recovery curves for PLys-FITC. The raw data (shaded grey), mean (dark blue) and 95% confidence limit (light blue) from 16 experiments are shown. The recovery profile was fit to a double exponential curve to obtain the diffusion coefficients $2.4 \pm 1.4 \mu\text{m}^2 \text{s}^{-1}$ and $0.4 \pm 0.17 \mu\text{m}^2 \text{s}^{-1}$.

Results and Discussion

Reversible formation of coacervates within lipid vesicles can be regulated by tuning pH.

To encapsulate coacervate forming components, GUVs were formed using the gel-assisted swelling methodology^[19] in the presence of polylysine (PLys) with either CM-Dextran or Adenosine Triphosphate (ATP) (Fig. 1A, Fig. S1). Coacervation was inhibited during vesicle formation by setting the pH above the pKa of PLys (pH 10.5) (Fig. 1B). At a pH above the pKa of PLys, the coacervate components do not interact with one another as the amine groups are deprotonated and are therefore unavailable for phase separation via electrostatic interactions. The GUVs were composed of a phospholipid, POPC, (1-palmitoyl-2-oleoyl-sn-glycero-3-phosphocholine), cholesterol, and a small fraction of fluorescent lipid dye - DiD (1,1'-

Diocetadecyl-3,3,3',3'-Tetramethylindodicarbocyanine, 4 Chlorobenzene-sulfonate salt) for visualisation of the membrane (see materials and methods). Vesicles were formed in the presence of a buffer solution containing HEPES (5 mM), sucrose (180-200 mM), PLys (40 mM) and ATP (10 mM), or PLys (40 mM) and CM-Dextran (10 mM) at pH 11, at room temperature in the dark. In order to visualise the coacervate components, the coacervate mixture was doped with 0.25% (v/v) FITC-tagged PLys, or FITC-tagged CM-Dextran. Fluorescent confocal microscopy images showed a population of lipid vesicles by fluorescence of the lipophilic dye, DiD, with FITC fluorescence distributed both inside and outside of the lipid vesicles from FITC-tagged PLys (Fig. S2). The vesicles were typically between 2-30

RESEARCH ARTICLE

μm in diameter, which is expected of GUVs produced via the gel-assisted swelling method. To ensure that coacervate microdroplets would only form within the vesicles, the GUV dispersions were washed with an iso-osmolar glucose solution at pH 11 to remove excess coacervate components from the outside of the vesicles (see materials and methods). Confocal microscopy images showed that the vesicles had been successfully washed as fluorescence intensity line profiles across the lipid vesicle, normalised to 1, showed a low level of fluorescence intensity on the outside of the lipid vesicles compared to before the wash step (Fig. 1Ci,ii and Fig. S2).

Next, we aimed to induce coacervation within the GUVs by lowering the pH below the pKa of PLys. The pH of the system was reduced to 9-8.5 by adding an iso-osmolar glucose buffer at pH 7.3. The final pH was confirmed by undertaking control experiments without GUVs where the same volume of pH 7 buffer was exchanged for pH 11 buffer and the pH measured. Confocal fluorescence images following the pH reduction showed initial formation of a number of small droplets inside the lipid vesicles with high FITC fluorescence intensity attributed to accumulation of FITC-tagged PLys (Fig. S3). These droplets fused together over time to produce a single highly fluorescent microdroplet within each individual lipid vesicle (Fig. S3, and Fig. 1Di,ii). This process of nucleation and growth is characteristic of coacervate formation within lipid vesicles or within water-oil emulsions^{[7],[8]} and occurred on the order of tens of minutes (Fig. S3). It is interesting to note that line profiles show no fluorescence intensity from the lipid dye, DiD, within the PLys-rich droplets and no FITC fluorescence within the lipid membrane (Fig. 1Di,ii). This shows that the coacervate microdroplet is a distinct and separate sub-compartment within the lipid vesicle as there is no cross-contamination of the lipid within the coacervates. After formation, the PLys rich droplets and lipid vesicles remain stable for at least one day (Fig. S4).

We next aimed to test whether coacervation within GUVs is reversible by increasing the pH to above the pKa of pLys. At this pH the amine group is deprotonated and electrostatic interactions between the coacervate components are annulled (Fig. 1A). To do this, we increased the pH by exchanging the outer vesicular solution for an iso-osmolar glucose buffer at pH 11 and observed that the coacervation process within the GUVs is completely reversible. Confocal fluorescence images showed a transition of the FITC fluorescence from a heterogeneous coacervate droplet, to a homogeneous distribution throughout the interior of the GUVs

upon increasing the pH of the dispersion to pH 11 as observed prior to the first pH switch (Fig. 1Ei,ii and Fig. S5).

To confirm that PLys rich droplets, at pH 9, were indeed fluid coacervate microdroplets, fluorescence recovery after photobleaching (FRAP) of FITC-tagged PLys within the microdroplets in the hybrid protocells was undertaken (Fig. 1F, Fig. S6). FRAP data was normalised for bleaching and the whole coacervate droplet showed a 100 % fluorescence recovery which is characteristic of the microdroplets and attributed to the liquid-like and dynamic behaviour of coacervates^{[20],[21]}. In addition, fitting the recovery profile to a double exponential gave two time constants, τ , of 0.19 ± 0.12 s and 3.07 ± 6.6 s and diffusion coefficients of $2.4 \pm 1.4 \mu\text{m s}^{-1}$ and $0.4 \pm 0.17 \mu\text{m s}^{-1}$ respectively (Fig. 1G) (see materials and methods). The FRAP recovery and the measured diffusion coefficients are on the same order of magnitude as those obtained from coacervate microdroplets formed in the absence of lipid vesicles. This confirmed that the microdroplets formed within the GUVs triggered by changes in pH are indeed characteristic coacervate droplets^{[20],[21],[22]}.

To further validate that coacervation was taking place between the PLys and its counter charged electrolyte as described, we undertook the same encapsulation and pH switch methodology but with PLys alone (in the absence of ATP) within the lipid vesicle. At pH 11 the PLys was diffuse and evenly distributed throughout the GUV. Upon acidification to pH 9, there was no change in the distribution of dye (Fig. S7). This data confirmed that the liquid droplets formed via electrostatic interactions and subsequent phase separation between PLys and its counter molecule (ATP).

Taken together, these results demonstrate that our methodology can be used to reversibly tune the formation and dissolution of a single PLys/ATP coacervate microdroplet within a GUV. The fact that these hybrid protocells are stable for at least a day suggests that these platforms can also be used to support enzymatic reactions.

Dynamic compartmentalisation facilitates enzymatic activity. To determine whether *in situ* dynamic compartmentalisation could support and tune enzymatic reactions, we examined the activity of formate dehydrogenase in our system. In this well-established assay, formate dehydrogenase oxidises formate to carbon dioxide, with the concomitant reduction of NAD⁺ to fluorescent NADH. It has previously been shown that coacervate microdroplets will

RESEARCH ARTICLE

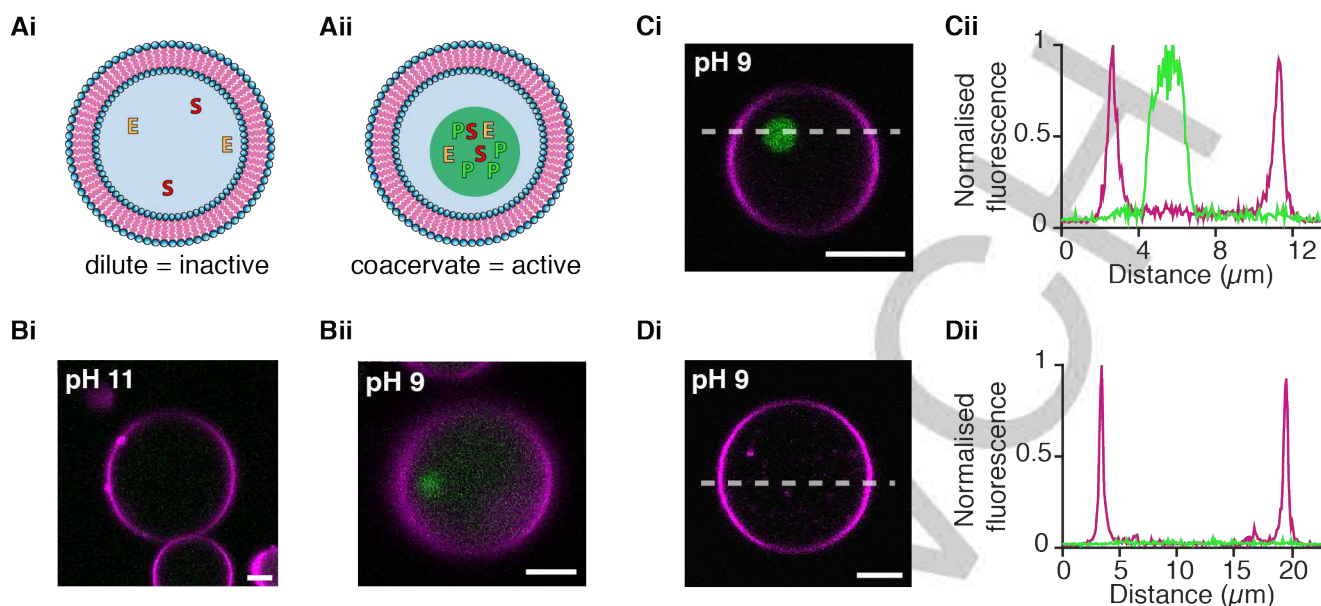


Figure 2. Activation of formate dehydrogenase enzyme reaction in lipid vesicles through pH triggered coacervation. (A) Schematics depicting activation of an enzyme by *in situ* coacervation and molecular up-concentration into the membrane-free droplet, E represents enzyme, S: substrate and P: Product (Ai) low concentration of enzyme means that the reaction is too dilute and no activity is observed (Aii). In the presence of a coacervate the enzyme and substrates are up-concentrated into the coacervate and the reaction is initiated (B) Fluorescent confocal microscopy images showing the activity of formate dehydrogenase at 0.1 U mL⁻¹ in GUVs upon coacervation at pH 9. (Bi) No NADH fluorescence is observed within the GUV containing PLYs/ATP at pH 11. (Bii) After switching the pH to 9 and 24 hrs of incubation at room temperature fluorescence from NADH was observed within the PLYs/ATP coacervate and in the surrounding aqueous solution within the lipid vesicle. Scale bar = 5 μm. (C,D) At low concentration of formate dehydrogenase (0.005 U mL⁻¹), sodium formate (5 mM) and β-NAD⁺ (0.45 μM) the enzyme is active only in the presence of a coacervate and subsequent up-concentration. Confocal microscopy images (i) and corresponding line profiles (ii) after 24 hours of incubation at room temperature. (C) GUVs containing PLYs/ATP and the enzyme show increased NADH fluorescence within the coacervate droplet. (D) GUVs without PLYs/ATP coacervates showed no presence of NADH fluorescence at pH 9. Both GUVs were treated with the same pH switching methodology as previously described. Scale bar = 5 μm.

partition and up-concentrate a range of substrates and molecules^{[23],[24]}. Therefore, we wondered whether inducing coacervation could alter enzymatic reactions via the up concentration of enzyme reactants within the coacervate droplet as previously observed with aqueous two phase systems^[25] (Fig. 2A).

Firstly, we probed the effect of *in situ* compartmentalisation on the enzyme formate dehydrogenase. FITC-labelled formate dehydrogenase (0.1 U mL⁻¹) was co-encapsulated within POPC: cholesterol vesicles and the coacervate components at pH 11, as previously described. On reducing the pH to pH 9, we observe a change in the distribution of dye within the GUVs from a homogeneous distribution throughout the interior of the vesicle to a heterogeneous distribution within the GUV by confocal microscopy. There was a region of high fluorescence intensity associated to the coacervate microdroplet, with no observable fluorescence intensity in the aqueous media surrounding the coacervate within the lipid vesicle (Fig. S8). Our results are in agreement with previous studies where formate dehydrogenase and other molecules partition and up-concentrate into preformed

coacervate droplets. This shows that molecular encapsulation within lipid vesicles, washing and consequent pH changes does not alter the ability for coacervates to incorporate client molecules such as enzymes. To ensure that formate dehydrogenase was active after the pH switch, dynamic hybrid protocells were produced as discussed previously but with the addition of the formate dehydrogenase (0.1 U mL⁻¹); the substrate, formate (5mM); and the cofactor, β-NAD⁺ (0.45 mM). Confocal images after 24 hrs show NADH fluorescence intensity distributed throughout the GUV with an increase of fluorescence intensity within the GUV and the coacervate microdroplet (Fig. 2Bi,ii). Our results, along with control experiments (Fig. S9), confirm that formate dehydrogenase is active at pH 9 and after a pH switch.

Building on our results, we wanted to exploit *in situ* coacervation as a means to activate the formate dehydrogenase reaction by the up-concentration of the reactants into the coacervate droplet (Fig. 2A). Control experiments had shown that NADH production within lipid vesicles, in the absence of coacervate forming components, was dependent on the concentration of formate dehydrogenase. End-point

RESEARCH ARTICLE

measurements showed that at low concentrations of formate dehydrogenase (0.005 U mL^{-1}) there was no NADH production, after 24 hrs, compared to increased concentrations of formate dehydrogenase ($0.1, 0.05 \text{ U mL}^{-1}$) (Fig. S10). We therefore encapsulated formate dehydrogenase (0.005 U mL^{-1}) with formate (5 mM) and $\beta\text{-NAD}^+$ (0.45 mM) into POPC/cholesterol vesicles with and without PLys and ATP, at pH 11 to determine whether up-concentration of formate dehydrogenase into the coacervate droplet would switch on the production of NADH. Following our established methodology, the two populations of vesicles were washed and coacervation was triggered by a reduction in pH to pH 9. After 24 hours, vesicles with and without coacervates were characterised for NADH production. Confocal fluorescence microscopy images showed high fluorescence intensity associated with NADH within the coacervate droplet encapsulated within the vesicle but no NADH fluorescence within the vesicles without coacervate microdroplets (Fig. 2C,D). The data suggests that pH triggered coacervation within lipid vesicles can turn on enzymatic reactions by the up-concentration of materials into the coacervate reaction centre. Despite this, we wanted to rule out the possibility of enzyme leakage from the interior of the lipid vesicle. If formate dehydrogenase was leaving the coacervate droplet then the production of NADH within the vesicle would be reduced. Control experiments of encapsulated formate dehydrogenase within GUVs showed no decrease in fluorescence from FITC-tagged formate dehydrogenase within the lipid vesicle (Fig. S11). This supports our observations that NADH was produced by the up-concentration of the enzyme assay by *in situ* compartmentalisation.

To confirm that coacervate microdroplets are able to switch on reactions by molecular up-concentration, we compared the production of NADH as a function of time in coacervate dispersions and in buffer at the same molecular concentrations, in the absence of lipid vesicles. To do this, solutions comprised of formate dehydrogenase (0.002 U mL^{-1}), formate (25 mM) and $\beta\text{-NAD}^+$ (0.6 mM) were prepared with and without PLys and ATP (40 mM and 10 mM respectively) in HEPES buffer (5 mM) at pH 11. The reaction mixtures were incubated for 30 minutes at pH 11, after which the pH was switched to 9 and NADH production was measured using fluorescence spectroscopy (Fig. S12). Our results show that NADH was produced within the coacervate dispersions but not in the buffer solution. These results confirm that at low concentrations of formate dehydrogenase, coacervate droplets can switch on enzymatic activity by up-concentration. Taken together, our results show that pH triggered coacervation

within lipid vesicles can activate dormant enzymatic reaction through the up-concentration of molecules into the coacervate reaction centre.

Formation of hybrid protocells are robust. Having shown that *in situ* coacervation by pH switching can activate the formate dehydrogenase reaction by up-concentration, we assessed the reproducibility of our protocol for the *in situ* coacervation in lipid vesicles for both PLys/ATP and CM-Dextran/PLys coacervates. The methodology is readily transferrable to other coacervate forming systems such as CM-Dextran/PLys (Fig. S13) by exploiting the inherent pH responsiveness of PLys. Image analysis of confocal cross sections of GUVs encapsulating PLys/ATP or CM-Dextran/PLys droplets was undertaken by using a custom written image analysis routine in FIJI. Segmentation of hundreds of lipid vesicles and coacervates (Fig. 3A) which had been generated by a change in pH switch showed that 17 and 41% of the GUVs were occupied by coacervates in the case of CM-Dextran coacervates (Fig. 3A) and 24% in the case of ATP based coacervates (Fig. 3B).

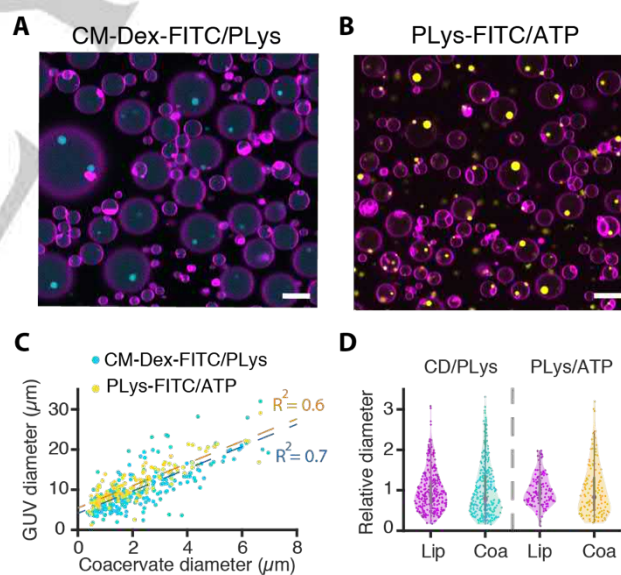


Figure 3. Size characterization of PLys/ATP and CM-Dextran/PLys coacervates formed in GUVs. (A) Fluorescence confocal cross sections of lipid vesicles containing CM-Dextran/PLys coacervates with FITC-tagged CM-Dextran ($0.5\% \text{ (v/v)}$) (B) Confocal cross sections of GUVs containing PLys/ATP coacervates with FITC-tagged PLys ($0.25\% \text{ v/v}$) at pH 9. Scale bars = $10 \mu\text{m}$. (C) Scatter plot of coacervate diameters plotted against vesicle diameters. Data shows a correlation between the size of the vesicle and the internal coacervate. Straight lines fitted to the data and gave R^2 values of 0.6 (PLys/ATP) and 0.7 (CM-Dextran/PLys). (D) Violin plot of the relative diameters of each population show that the relative spread in size variation is similar for both lipid vesicles and coacervates, and between the two populations, when normalized for the mean size.

RESEARCH ARTICLE

Determination of the vesicle and droplet diameters was carried out using FIJI image analysis, only for the GUVs which contained coacervate droplets. The diameters of lipid vesicles varied from 2-30 μM with the diameters of the coacervates ranging from 0.2 - 8 μM . For the CM-Dextran based system $d_{\text{GUV}} = 10.4 \pm 5.4 \mu\text{m}$, $d_{\text{CM-Dextran/PLys}} = 2.3 \pm 1.5 \mu\text{m}$, $n > 300$ (Fig. S14A) and for the ATP based coacervates the mean diameter and standard deviation was $d_{\text{GUV}} = 11.2 \pm 4.2 \mu\text{m}$, $d_{\text{PLys/ATP}} = 2.1 \pm 1.3 \mu\text{m}$, $n > 120$ (Fig. S13B). The relative standard deviations (RSD) were comparable between the two systems where the CM-Dextran system varied by 65 % and 52 % for the vesicles and the coacervates respectively and for the ATP based system the vesicles and coacervates had a coefficient of variation of 62 % and 38 % respectively.

For those GUVs which contained coacervates, the R^2 value from a linear fit of the vesicle diameter vs the coacervate diameter were 0.8 and 0.7 for the CM-Dextran/PLys and 0.6 for the PLys/ATP systems respectively (Fig. 3C, Fig. S15). These results show that for those lipid vesicles which do encapsulate the polymers there is a correlation to the size of the coacervate droplets and the size of the GUVs. This is most likely attributed to the vesicle volume, that reflects the amount of material encapsulated and therefore the size of the coacervate. Furthermore, the variance in the populations of the vesicles and coacervates were compared by normalising the diameters to the mean diameter of the population. The violin plots show that the spread of data between lipid vesicles sizes and their coacervates was very similar for both the PLys/ATP and CM-Dextran/PLys system (Fig. 3D).

The apparent low encapsulation of 17 and 40 % of coacervates could be attributed to out of plane coacervates that were not captured in confocal cross-sections. Therefore, additional experiments were undertaken to capture the full z-volume of the lipid vesicles using a spinning disk confocal microscope to generate maximum projections of lipid vesicles with PLys/ATP coacervates (see materials and methods and Fig. S16). The results showed the presence of coacervates in 100% of GUVs. In addition, the size analysis of maximum projections of lipid vesicles and coacervates gave the same diameters, within error, compared to analysis obtained from confocal cross-sections (Fig. S16).

Taken together, our analysis shows our methodology is reproducible and applicable to different coacervate systems provided one of the two components has a pH dependent moiety. In addition, the size of the coacervate droplet is directly influenced

by the size of the encapsulating vesicle. Despite the clear reproducibility of the methodology, we sought to improve upon the size distribution of the vesicle and corresponding coacervate droplets by using microfluidic techniques.

Microfluidic production of hybrid protocells. Microfluidic methodologies would enable us to produce monodisperse vesicles encapsulating coacervates with higher reproducibility and lower variance in size in a high throughput manner. Additionally, a microfluidic approach uses distinct solutions inside and outside the GUVs during formation, which then removes subsequent wash steps required in our bulk methodology. We used double-emulsion based microfluidics to generate lipid vesicles which contain dissolved coacervate components at pH 11. The device was made from PDMS using standard soft lithography methods and had a double cross junction geometry^[26] (see materials and methods) (Fig. 4Ai,ii) with channel heights of 50 μm .

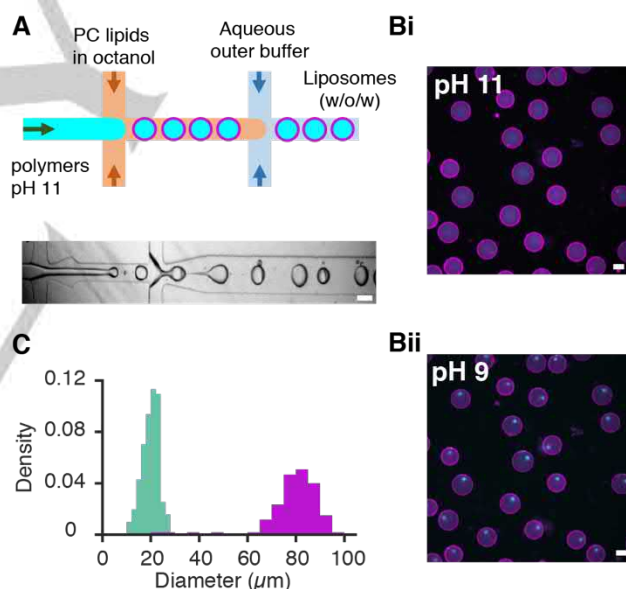


Figure 4. Formation of pH triggered coacervation in GUVs formed using microfluidics (A) A double cross junction device was used to produce Egg PC lipid vesicles containing diffuse PLys and ATP (4:1 molar ratio) at pH 11. The corresponding brightfield image of lipid vesicle production at the two junctions is also shown. Scale bar = 100 μm . **(B)** Fluorescence microscopy images showing (i) GUVs encapsulating PLys and ATP at pH 11. Cyan fluorescence from FITC-tagged PLys (0.25 %) and magenta from Texas Red DHPE membrane dye (0.1 %). (ii) GUVs containing coacervate microdroplets after a reduction in pH to pH 9, after 15 hrs. The concentrated PLys-FITC fluorescence is indicative of the formation of coacervate droplets. Scale bar = 50 μm . **(C)** Size quantification of the lipid vesicles (mean diameter = 80 $\mu\text{m} \pm 12 \mu\text{m}$, $n > 220$) and their encapsulated coacervates (mean diameter = 20 $\mu\text{m} \pm 12 \mu\text{m}$, $n > 220$). 100 % encapsulation efficiency was achieved.

RESEARCH ARTICLE

Sucrose/HEPES buffer containing diffuse PLys and ATP at pH 11 were flown through the inner aqueous channel to generate water-in-oil (w/o) emulsions with Egg PC lipids dissolved in 1-octanol. The first junction (width 50 μm) with a constricted opening facilitates a seamless pinching-off process to generate w/o droplets stabilised by Egg PC and Pluronic acid

The w/o droplets containing non-coacervated PLys and ATP were converted to a water-in-oil-in water (w/o/w) double emulsion droplets at the second junction, which is surface modified and has an aqueous fluid channel of 150 μm width (see materials and methods). This assists in efficient wetting of the second junction by co-flowing with the outer aqueous solution of the glucose/HEPES buffer at pH 11 (Fig. 4Bi). Coacervation was triggered with the addition of iso-osmotic pH 7.3 glucose buffer (Fig. 4Bii). Coacervates formed over a 15 h period (Fig. S17). Using this device, we achieved a 100 % encapsulation efficiency (Fig. S18), which has not been possible using other microfluidic approaches^[7]. The lipid vesicles produced were larger and more homogeneous in size compared to the swelling methodology ($d_{\text{GUV}} = 79.1 \pm 11.9 \mu\text{m}$) with a relative standard deviation (RSD) of 15%. The size variation of the coacervate droplets was also reduced compared to bulk methodologies (RSD>50%), with the $d_{\text{coac}} = 20.0 \pm 3.4 \mu\text{m}$ and a RSD of 17% (Fig. 4C) as expected by microfluidic techniques. We have therefore shown that *in situ* coacervation can be triggered in GUVs prepared by droplet-based microfluidics by an external change in pH. The applicability of the pH switch in droplet-based microfluidics demonstrates the use of the pH trigger across multiple experimental set ups.

Conclusion

In conclusion, we have presented a robust and reproducible methodology for the tuneable formation of liquid-liquid phase separated droplets within giant unilamellar vesicles. By exploiting the intrinsic pKa of cationic PLys we have generated a responsive system where phase separation is triggered through an external reduction in pH. We have further shown that we can utilise the sequestration properties of coacervate droplets for the dynamic *in situ* activation of enzymatic reactions. This represents a synthetic model for understanding the role of dynamic membrane-free sub-compartmentalisation in biological systems. In addition, our methodology is reproducible using bulk and microfluidic methodologies. Overall our system demonstrates a step forward in the design of multi-compartment synthetic cells, which are dynamically responsive to external stimuli. Such a dynamic

system will be of interest in the development of more complex synthetic cells and as minimal models for liquid-liquid phase separation in biological systems.

Acknowledgements

We acknowledge financial support from the MaxSynBio Consortium (jointly funded by the Federal Ministry of Education and Research (Germany) and the Max Planck Society); and the MPI-CBG. TYDT acknowledges the Cluster of Excellence Physics of Life of TU Dresden and EXC-1056 for funding. We acknowledge the Light Microscopy Facility and the Scientific Computing Facility at the MPI-CBG for assistance; Christoph Zechner for discussions regarding data analysis; Juan M. Inglesias-Artola and Björn Drobot for assistance with the FRAP analysis code; and Anatol W. Fritsch for assistance with undertaking spinning disk confocal microscopy experiments with the Olympus IXplore IX83 microscope.

Conflict of interest: The authors declare no conflict of interest

Materials and methods: All materials and methods are provided in the supplementary information

Key words: pH responsive, liquid-liquid phase separation, coacervates, lipid vesicles, active droplets, microfluidics, dynamic hybrid protocells

References:

- [1] T. M. Franzmann, M. Jahnel, A. Pozniakovsky, J. Mahamid, A. S. Holehouse, E. Nüske, D. Richter, W. Baumeister, S. W. Grill, R. V Pappu, et al., *Science* **2018**, 359, eaao5654.
- [2] T. J. Nott, T. D. Craggs, A. J. Baldwin, *Nat. Chem.* **2016**, 8, 569–575.
- [3] S. Koga, D. S. Williams, A. W. Perriman, S. Mann, *Nat. Chem.* **2011**, 3, 720–724.
- [4] K. K. Nakashima, J. F. Baaij, E. Spruijt, *Soft Matter* **2018**, 14, 361–367.
- [5] N. Martin, L. Tian, D. Spencer, A. Coutable-Pennarun, J. L. R. Anderson, S. Mann, *Angew. Chemie Int. Ed.* **2019**, 58, 14594–14598.
- [6] R. Dimova, *Annu. Rev. Biophys.* **2019**, 48, 93–119.
- [7] N. N. Deng, W. T. S. Huck, *Angew. Chemie - Int. Ed.* **2017**, 56, 9736–9740.

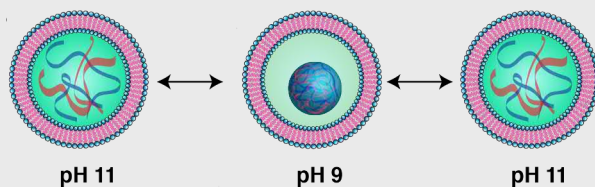
RESEARCH ARTICLE

- [8] S. Deshpande, F. Brandenburg, A. Lau, M. G. F. Last, W. K. Spoelstra, L. Reese, S. Wunnava, M. Dogterom, C. Dekker, *Nat. Commun.* **2019**, *10*, 1800.
- [9] R. Booth, Y. Qiao, M. Li, S. Mann, *Angew. Chemie Int. Ed.* **2019**, *58*, 9120–9124.
- [10] M. S. Long, C. D. Jones, M. R. Helfrich, L. K. Mangeney-Slavin, C. D. Keating, *Proc. Natl. Acad. Sci. U. S. A.* **2005**, *102*, 5920–5925.
- [11] Y. Li, R. Lipowsky, R. Dimova, *J. Am. Chem. Soc.* **2008**, *130*, 12252–12253.
- [12] E. Sokolova, E. Spruijt, M. M. K. Hansen, E. Dubuc, J. Groen, V. Chokkalingam, A. Piruska, H. A. Heus, W. T. S. Huck, *Proc. Natl. Acad. Sci. U. S. A.* **2013**, *110*, 11692–7.
- [13] N. Yandrapalli, T. Robinson, *Lab Chip* **2019**, *19*, 626–633.
- [14] J. Crosby, T. Treadwell, M. Hammerton, K. Vasilakis, M. P. Crump, D. S. Williams, S. Mann, *Chem. Commun.* **2012**, *48*, 11832.
- [15] J. B. Woodruff, B. Ferreira Gomes, P. O. Widlund, J. Mahamid, A. Honigmann, A. A. Hyman, *Cell* **2017**, *169*, 1066–1077.e10.
- [16] J. Wang, J. M. Choi, A. S. Holehouse, H. O. Lee, X. Zhang, M. Jahnel, S. Maharana, R. Lemaitre, A. Pozniakovsky, D. Drechsel, et al., *Cell* **2018**, *174*, 688–699.e16.
- [17] S. F. Banani, H. O. Lee, A. A. Hyman, M. K. Rosen, *Nat. Publ. Gr.* **2017**, *18*, 285–298.
- [18] M. C. Munder, D. Midtvedt, T. Franzmann, E. Nüske, O. Otto, M. Herbig, E. Ulbricht, P. Müller, A. Taubenberger, S. Maharana, et al., *Elife* **2016**, *5*, DOI 10.7554/eLife.09347.
- [19] A. Weinberger, F.-C. Tsai, G. H. Koenderink, T. F. Schmidt, R. Itri, W. Meier, T. Schmatko, A. Schröder, C. Marques, *Biophys. J.* **2013**, *105*, 154–64.
- [20] B. Drobot, J. M. Iglesias-Artola, K. Le Vay, V. Mayr, M. Kar, M. Kreysing, H. Mutschler, T.-Y. D. Tang, *Nat. Commun.* **2018**, *9*, 3643.
- [21] W. M. Aumiller, F. Pir Cakmak, B. W. Davis, C. D. Keating, *Langmuir* **2016**, *32*, 10042–10053.
- [22] S. Banjade, M. K. Rosen, *Elife* **2014**, *3*, DOI 10.7554/eLife.04123.001.
- [23] T.-Y. D. Tang, M. Antognozzi, J. A. Vicary, A. W. Perriman, S. Mann, *Soft Matter* **2013**, *9*, 7647.
- [24] N. Martin, M. Li, S. Mann, *Langmuir* **2016**, *32*, 5881–5889.
- [25] C. A. Strulson, R. C. Molden, C. D. Keating, P. C. Bevilacqua, *Nat. Chem* **2012**, *4*, 941.
- [26] J. Petit, I. Polenz, J.-C. Baret, S. Herminghaus, O. Bäumchen, *Eur. Phys. J. E* **2016**, *39*, 59.

RESEARCH ARTICLE

Entry for the Table of Contents (Please choose one layout)

RESEARCH ARTICLE



Celina Love,^[a] ^[b] Jan Steinküler,^[c] David
Gonzales,^[a] ^[b] ^[c] Naresh Yandrapelli,^[d]
Tom Robinson,^[c] Rumiana Dimova,^[d]
T-Y Dora Tang*^[a] ^[b]

Page No. – Page No.

**Reversible pH responsive coacervate
formation in lipid vesicles activates
dormant enzymatic reactions**

Abstract, Introduction, Results and discussion, Figure 1-4, Conclusion, Acknowledgements, References

Accepted Manuscript

Supporting Information

©Wiley-VCH 2016

69451 Weinheim, Germany

Reversible pH responsive coacervate formation in lipid vesicles

Celina Love,^{[a] [b]} Jan Steinküler,^[d] David T. Gonzales,^{[a] [b] [c]} Naresh Yandrapalli,^[d] Tom Robinson,^[d]
Rumiana Dimova,^[d] T-Y Dora Tang^{*[a] [b]}

Abstract: *In situ*, reversible coacervate formation within lipid vesicles represents a key step in the development of responsive synthetic cellular models. Here we exploit the pH responsiveness of a polycation above and below its pKa, to drive liquid-liquid phase separation to form single coacervate droplets within lipid vesicles. The process is completely reversible as coacervate droplets can be disassembled by increasing the pH above the pKa. We further show that pH triggered coacervation in the presence of low concentrations of enzymes activate dormant enzyme reactions by molecular up-concentration into the coacervate droplets. In conclusion, this work establishes a tuneable, pH responsive, enzymatically active multi-compartment synthetic cell. The system is readily transferred into microfluidics, making it a robust model for addressing general questions in biology such as the role of phase separation and its effect on enzymatic reactions using a bottom-up synthetic biology approach.

DOI: 10.1002/anie.2016XXXXX

Table of Contents

1. Experimental Procedures	2
1.1. General reagents	2
1.2. Inner and outer solutions for swelling of Giant Unilamellar Vesicles	
1.3. Preparation of lipid Vesicle with encapsulated coacervate polymers	2
1.4. Reversible in-situ formation of coacervates within lipid vesicles triggered by pH	3
1.5. Preparation of FITC tagged enzymes	3
1.6. Activity of Formate dehydrogenase bulk coacervate dispersions	3
1.7. Activity of Formate dehydrogenase in lipid vesicles	3
1.8. Optical imaging of lipid vesicles	3
1.9. Fluorescence recovery after photo bleaching	4
1.10. Microfluidics	4
2. Supplementary figures	

1. Experimental Procedures

1.1. General reagents

Poly-L-lysine hydrobromide (PLys, $(C_6H_{12}N_2O)_n$, 4 – 15 kDa, monomer Mw = 208.1 g mol⁻¹), carboxymethyl-dextran sodium salt (CM-Dex, $(C_6H_{10}O_5)_n$.(COOH), 10-20 kDa, monomer Mw = 191.3 g mol⁻¹), FITC-CM Dextran ($(C_6H_{10}O_5)_n$.(COOH).(C₂₁H₁₁NO₅S), 4,000 g mol⁻¹), adenosine 5-triphosphate disodium salt hydrate (ATP, C₁₀H₁₄N₅Na₂O₁₃P₃, 551.1 g mol⁻¹), β-nicotinamide adenine dinucleotide hydrate (β-NAD⁺, C₂₁H₂₇N₇O₁₄P₂, 663.4 g mol⁻¹), sodium formate (HCOONa, 68.0 g mol⁻¹), formate dehydrogenase from *Candida boidinii* (FDH, 74 kDa), polyvinyl alcohol (PVA, 89,000 - 98,000 g mol⁻¹, 99% hydrolyzed), chloroform (CHCl₃, 119.38 g mol⁻¹), toluene (C₆H₅CH₃, 92.14 g mol⁻¹), hydrogen peroxide (H₂O₂, 30 wt.%, 34.01 g mol⁻¹), hydrochloric acid (37 wt.%, HCl, 36.46 g mol⁻¹), poly(sodium 4-styrenesulfonate (C₉H₇NaO₃S)_n, 70,000 g mol⁻¹), Egg PC (L-α-phosphatidylcholine, 99% TLC, in chloroform, 25 mg/ml, ~768 g mol⁻¹), 1-Octanol (CH₃(CH₂)₇OH), 130.23 g mol⁻¹, Polydiallyldimethylammonium chloride (PDADMAC, (C₈H₁₆CIN)_n 20% wt in H₂O, monomer Mw= 161 g mol⁻¹), Poly (4-styrenesulfonic acid) (PSS, 18% wt in H₂O, Mw=75000 g mol⁻¹) and cholesterol (C₂₇H₄₆O, 386.65 g mol⁻¹) were all purchased from Sigma Aldrich, Missouri, USA. Fluorescein isothiocyanate isomer I (FITC, C₂₁H₁₁NO₅S, 389.38 g mol⁻¹), Texas Red™ 1,2-Dihexadecanoyl-sn-Glycero-3-Phosphoethanolamine, Triethylammonium Salt (Texas Red™ DHPE, C₇₄H₁₁₇N₄O₁₄PS₂, 1 mM, 1381.8 g mol⁻¹), DiI_{C18(5)} solid(1,1'-Diocetadecyl-3,3',3'-Tetramethylindodicarbocyanine, 4 Chlorobenzene-sulfonate Salt (DiI, C₆₇H₁₀₃CIN₂O₃S, 1052.1 g mol⁻¹), Pluronic F-63 (Non-ionic surfactant x100, (C₃H₆O. C₂H₄O)_x, ~ 8400 g mol⁻¹) and sucrose (C₁₂H₂₂O₁₁, 342.3 g mol⁻¹) were purchased from Thermo Fisher Scientific, Massachusetts, USA. Glucose (C₆H₁₂O₆, 180.2 g mol⁻¹) and Sodium hydroxide (NaOH, 39.997 g mol⁻¹) were purchased from Merck, Kenilworth, USA. FITC-PLys ($(C_6H_{12}N_2O)_n$.(C₂₁H₁₁NO₅S), 25,000 g mol⁻¹) was purchased from Nanocs, New York, USA. 1-palmitoyl-2-oleoyl-sn-glycero-3-phosphocholine (POPC, C₄₂H₈₂NO₈P, 760.1 g mol⁻¹) was purchased from Avanti Polar Lipids, Alabama, USA. HEPES (C₈H₁₈N₂O₄S, 238.3 g mol⁻¹) was purchased from Roth, Karlsruhe, Germany. PDMS (SYLGARD®184 silicone elastomer kit) was purchased from Dow Corning, USA. Osmometer calibration samples (100, 300 mOsmol kg⁻¹) were purchased from Gonotec, Berlin, Germany. Picodent Twinsil speed was purchased from Picodent, Wipperfurth, Germany. All materials were used without further purification.

Milli-Q water was used to prepare aqueous stock solutions of PLys (200 mM, pH 8), ATP (100 mM, pH 8), CM-Dex (1 M, pH 8), FDH (10 un mL⁻¹), β-NAD⁺ (45 mM), sodium formate (0.5 or 1 M) and HEPES (5 mM, pH 7.3). The pH of all stocks was adjusted using a 10 M NaOH solution. Aqueous stock solutions including buffer were stored at -20 °C until use. Stock solutions of lipids POPC, Cholesterol and the dye DiI) were prepared in chloroform to a concentration of 4 mM and stored under argon at -20 °C until use. Glass slides were pegylated by leaving the slides in a stirred bath of toluene with PEGsilane (0.2 %), activated with concentrated HCL (0.08 %) overnight at room temperature. Slides were then washed with toluene, ethanol and then water and dried with compressed air.

1.2. Inner and outer solutions for swelling of giant unilamellar vesicles (GUVs)

Typical inner liposome solutions consisted of 3.5 - 5 mM HEPES, 180 - 200mM Sucrose and either PLys (40 mM), PLys (40 mM) and ATP (10 mM) or CM-Dextran (40 mM) and PLys (10 mM) with FITC tagged PLys (0.25% v/v). For experiments with the enzyme formate dehydrogenase (Fig. 5), reactants were added to the inner solution to final concentrations of either 0.1 or 0.005 un mL⁻¹ (FDH), 4 mM (sodium formate) and 0.45 μM (β-NAD⁺). All inner solutions were prepared at pH 11 by addition of 10 mM NaOH. Final

SUPPORTING INFORMATION

osmolarities ranged between 200 to 240 mOsmol kg⁻¹. The osmolarity of the solution was measured with a cryoscopic osmometer, Osmomat 030 (Gonotec, Berlin, Germany) by freezing point depression.

Typical outer solutions consisted of HEPES (2-5 mM) and glucose (200 – 240 mM) adjusted to either pH 11 (wash solution) or pH 7.3 (trigger solution) with 10 M NaOH solution. The osmolarity was adjusted using either a 2.5 M glucose solution or water, to be within + 5 mOsmol kg⁻¹ of the inner solution.

1.3. Preparation of GUVs with encapsulated coacervate polymers

Giant vesicles were prepared by hydration of a lipid film dried onto a PVA film as described previously with minor modifications¹. Glass microscope slides were cleaned with ethanol and water and then dried thoroughly with air. 50 μ L of a 4% (w/v) PVA solution in Milli-Q water was then spread onto three-quarters of a glass microscope slide using a pipette tip and then incubated on a hot plate at 40 °C for 20 mins to dry the PVA. The temperature of the hot plate was then increased to 55 °C for another 10 minutes to ensure that the PVA film was completely dry. 2.5 μ L of a 4 mM lipid/chloroform solution containing POPC:Cholesterol:DiD at a molar ratio of 90:9.7:0.3 respectively, was then distributed onto the PVA film using a glass Hamiltonian syringe by gently running it over the surface of the PVA. The slide was then left under vacuum for at least 1 hour to remove all of the chloroform.

A chamber was assembled around the dried lipid and PVA film by placing a 1 mm thick Teflon spacer on top of the PVA, then placing glass cover slip on top of the spacer and securing these with bulldog clips. The chamber was filled with approximately 600 μ L of the inner sucrose solution with the coacervate polymers and then left in the dark at room temperature for 30 mins, to allow hydration and swelling of the lipid film and the formation of lipid vesicles. GUVs were then harvested by gently tapping the bottom of the chamber, then careful pipetting the solution from the chamber into an Eppendorf tube. Typically, samples were used within 24 hours, but were stable at 4 °C for up to a month.

1.4. Reversible in situ formation of coacervates within lipid vesicles triggered by pH

100 μ L of the lipid vesicles solution was loaded into a chamber formed from an 8 well bottomless μ -Slide with a self-adhesive underside (Ibidi GmbH, Germany) attached to a PEGylated 24 x 60 mm glass cover slips. An additional 500 μ L of the wash solution (pH 11) was added to the GUV dispersion and gently pipetted to mix and then left for 15 mins to allow the lipid vesicles to settle to the bottom of the chamber. An additional 300 μ L of wash solution was added and left to equilibrate for 5 mins. The vesicles were then washed by exchanging the chamber solution with 200 μ L of the outer wash solution, at least 6 times, to remove excess coacervate polymers and reactants for the enzyme assay from the outer solution.

To trigger coacervation within the lipid vesicles, the same volume (typically 200 μ L) of wash solution (pH 11) was exchanged for the trigger solution (pH 7.3), exchange of the buffer was repeated at least twice (400 μ L) and up to four times (800 μ L). To initiate coacervate dissolution, the chamber solution was exchanged for the wash solution (pH 11) in the same way as coacervation formation.

1.5. Preparation of FITC tagged enzymes

Proteins were labelled with Fluorescein isothiocyanate (FITC) (10 mM in ethanol) using standard protocols. 10 mg of formate dehydrogenase was dissolved in 0.1 M sodium carbonate buffer (pH 9) at a concentration of 2 mg ml⁻¹. Whilst stirring the protein solution, FITC was added stepwise in 5 μ L aliquots to a final volume of 20 μ L for every 1 ml of protein solution. The solution was dialyzed for 2 hours in 5 mL of Milli-Q water, and then overnight in another 2 mL of Milli-Q to remove any excess FITC. The tagged dye was stored in aqueous solution at -20 °C until use.

1.6. Activity of formate dehydrogenase bulk coacervate dispersions

Enzyme activity was confirmed by observing formate dehydrogenase kinetics in dispersions of coacervate microdroplets. The enzyme reaction was prepared in 20 μ L of HEPES/Sucrose (5 mM/ 200 mM) buffer or in buffer with PLys:ATP coacervates (final coacervate concentration 40:10 mM). Final concentrations of reactants were 0.45 mM (β -NAD⁺), 5 mM (sodium formate) and 0.002 un ml⁻¹ (formate dehydrogenase). The reaction was initiated by the addition of the enzyme, mixed, and then loaded (20 μ L) into a 384 well plate (microplate, 693 PS, Small Volume, LoBase, Med. binding, Black, Greiner Bio-one). The kinetics of the reactions were recorded using TECAN Spark 20M well plate reader spectrophotometer (Tecan AG, Männedorf, Switzerland) by measuring the increase in NADH fluorescence over time ($\lambda_{\text{ex}} = 340$ nm and $\lambda_{\text{em}} = 460$ nm, 5 nm bandwidth at 25 °C).

1.7. Activity of formate dehydrogenase in GUVs

Following the protocol outlined above, the inner lipid vesicles solution was prepared with formate dehydrogenase, sodium formate and β -NAD⁺, to final concentrations of 0.005 un ml⁻¹, 5 mM and 0.45 μ M respectively, with and without coacervates. GUVs then underwent the same pH triggering methodology *via* washing as described and microscopy images were obtained immediately before pH switching and 24 hrs later.

1.8. Optical imaging of GUVs

Fluorescence confocal microscopy of GUVs was undertaken using a Zeiss LSM 880 Airy inverted laser scanning confocal microscope equipped with a Zeiss 40x/1.2 C-Apochromat DIC water immersion objective, a Zeiss 20x/0.8 Plan-Apochromat air objective and a 32 GaAsP PMT channel spectral detector. FITC labelled coacervates were imaged ($\lambda_{\text{FITC}} = 488$ nm) by the 488 nm laser and emission wavelengths detected at $\lambda_{\text{FITC}} = 495 - 579$ nm. The DiD labelled lipid membranes ($\lambda_{\text{DiD}} = 644$ nm) were excited with

SUPPORTING INFORMATION

a 633 nm laser for excitation and emission wavelengths detected at $\lambda_{\text{DiD}} = 652\text{-}695$ nm. NADH, the product of the formate dehydrogenase reaction ($\lambda_{\text{NADH}} = 340$ nm), was excited using a 355 nm DPSS UV laser and emission wavelengths detected at $\lambda_{\text{NADH}} = 420 - 500$ nm. Characterisation of GUVs and coacervate sizes was carried out with images obtained using the 40x lens. Fiji was used to obtain the fluorescence intensity across the GUVs using the line plot function for the DiD channels and the FITC channels. The fluorescence intensity of each of the channels was normalized to one. The images were further processed using a custom-made Fiji (Image J) macro that segmented GUV membranes and the coacervates inside them. The optical images were then further processed using MATLAB (Mathworks) to determine size of the vesicles or the coacervates. The correlated size distributions were fit to a linear regression model to calculate the R^2 values using MATLAB. The diameters were normalized by the mean to obtain the relative diameter.

1.9. Fluorescence recovery after photo bleaching

Fluorescence recovery after photobleaching (FRAP) experiments were undertaken for PLys/ATP coacervates microdroplets encapsulated in GUVs. All FRAP experiments were carried out using an Andor Eclipse Ti inverted spinning disk confocal microscope, equipped with a FRAPPA module and an Andor iXON 897 Monochrome EMCCD camera and imaged using a Nikon 60x/1.2 DIC Plan Apochromat VC water immersion objective. Bleaching of the droplet was achieved using a 405 nm diode laser at 100% power. Imaging was carried out using a 488 nm DPSS laser for excitation of the FITC dye at $\lambda_{\text{FITC}} = 488$ with an emission wavelength of $\lambda_{\text{FITC}} = 500\text{-}590$ nm. Due to the fast recovery of the coacervates, a reduced frame size of 4 x 512 dexels was used so that a higher temporal resolution could be achieved. For each experiment, 20 pre-bleach images were acquired before bleaching. The fluorescence recovery was then recorded by imaging for 3 mins at 4 frames msec⁻¹ in the FITC channel only.

A custom written FIJI script was used to extract raw fluorescence data which was then normalized against a background region, a reference droplet and by the total fluorescence of the whole bleached droplet²⁻⁴. Using a custom MATLAB script, recovery profiles were fit to a double exponential curve using Eq. 1 to obtain the time constants τ_1 and τ_2 .

(1)

$$f(t) = \begin{cases} 1 & t < t_0 \\ 1 - A1 \exp\left(-\frac{t-t_{\text{bleach}}}{\tau_1}\right) + A2 \exp\left(-\frac{t-t_{\text{bleach}}}{\tau_2}\right) + C & t \geq t_0 \end{cases}$$

where t_0 is the first time point after bleaching, A1 and A2 are exponential prefactors, t is the time and t_{bleach} is the time of bleaching. The time constants were calculated from at least 16 bleaching events from at least two different samples. Fitted time constants were then converted to diffusion constants using Eq. 2⁵, where r is the radius of the bleach spot.

(2)

$$D = \frac{0.88r^2}{4\tau \ln 2}$$

1.10. Microfluidics

Giant vesicles were produced using a microfluidic chip design with two consecutive cross-junctions in a flow-focusing configuration that generates w/o/w double emulsion droplets. This design was based on the work published by Petit et al⁶ and fabricated in the Robinson Lab using standard lithography methodologies. Briefly, PDMS and curing agent (Sylgard 184, Dow Corning) were mixed in a 9:1 ratio, degassed for 30 min and poured on top of the silicon wafer to a height of 5 mm in a petri dish. The PDMS was further degassed for 10 min and cured in an oven at 90 °C for 3 hrs. After which the PDMS was left to cool to room temperature and peeled from the wafer. Inlets were generated by punching holes using 1 mm biopsy puncher (Kai Europe GmbH) and then bonded to glass slides which has been cleaned with ethanol and water. For successful bonding, both the glass coverslips and PDMS slices were treated with an air plasma at 0.6 bar for a period of one minute using plasma cleaner (PDC-002-CE, Harrick Plasma). Microfluidic chips were kept on a hot plate at 60°C for 2h to complete the bonding process before further use. All channels were 50 μm in height. The outer solution channels of the microfluidic chip were hydrophilized by oxidizing the channels by flushing with a 3:1 mix of 30 wt.% H₂O₂ and 37 wt.% HCl for 5 mins and then treating the channels with 5 vol.% PDADMAC and 2 vol.% poly(sodium 4-styrenesulfonate) for 2 mins each with water washes in between.

The microfluidic chips were loaded onto a Zeiss Axiocvert 200M inverted widefield microscope equipped with a 16 channel CoolLED pE-300-W and ANDOR ZYLA fast sCMOS camera and imaged using 10x air objective (10x/0.3 Plan-Neofluar, Air, Ph1, Zeiss). FITC was imaged using a 470nm broad spectrum LED for excitation through a GFP/Alexa 488/FITC filter set (excitation bandpass 449-489 nm, dichroic longpass 497nm, emission bandpass 502-549 nm). Texas Red DHPE in the lipid membrane was imaged using a 550nm broad spectrum LED for excitation through a ROX filter set (excitation bandpass 575±15 nm, beam splitter HC BS 596, emission bandpass 641±75). The three fluid phases were controlled using three MitoS pressure pumps (Dolomite, Royston, UK). Target pressures were 70-80-100 mbar for the inner-middle-outer solutions respectively. The inner solution and the outer solution have been described previously with the addition of 2% pluronic in the outer solution at pH 11, the middle solution was an oil phase comprised of EggPC lipids at a final concentration of 6.5 mM dissolved in 1-Octanol with 0.008 mM Texas Red DHPE. Lipids were prepared by

SUPPORTING INFORMATION

drying the required volumes of stock solution of EggPC dissolved in chloroform (25mg/ml) and Texas RED DHPE dissolved in chloroform (1mM) in a glass test tube under nitrogen for 15 mins, then left under vacuum for 1 hour. Solutions were dissolved in 1.5 mL of 1-octanol by sonicating at 37°C in a water bath for 1 hour. Solutions were stored at room temperature and used within 24 hours.

The vesicles were collected into micro-centrifuge tubes after formation and then pipetted onto homemade capillary slides formed from a 22x22 mm BSA coated cover slips mounted onto a parafilm channel on a 22 x 75 mm microscope slide. 15 μ L of the GUV dispersion were loaded into the chamber, imaged using fluorescence widefield microscopy as described previously. Coacervation was initiated by flushing at least 7 μ L of pH 7 buffer into the channel as described previously. The capillary channel was sealed completely with Picodent Twinsil speed curing silicone and images were taken every 5 minutes for 15 hours. Image analysis was undertaken using FIJI and custom written code as described previously.

2.0 Supplementary figures

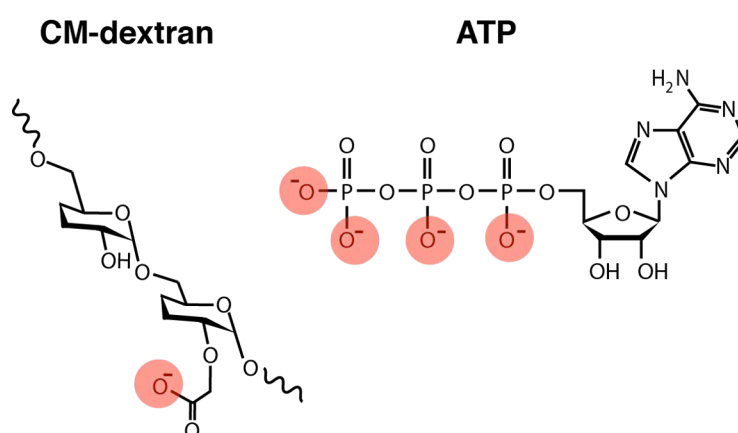


Figure S1. Chemical structures of the negatively charged coacervate molecules, carboxymethyl-Dextran (CM-Dextran) and Adenosine triphosphate (ATP) that undergo electrostatic attraction and coacervation with the PLys at pH 9.

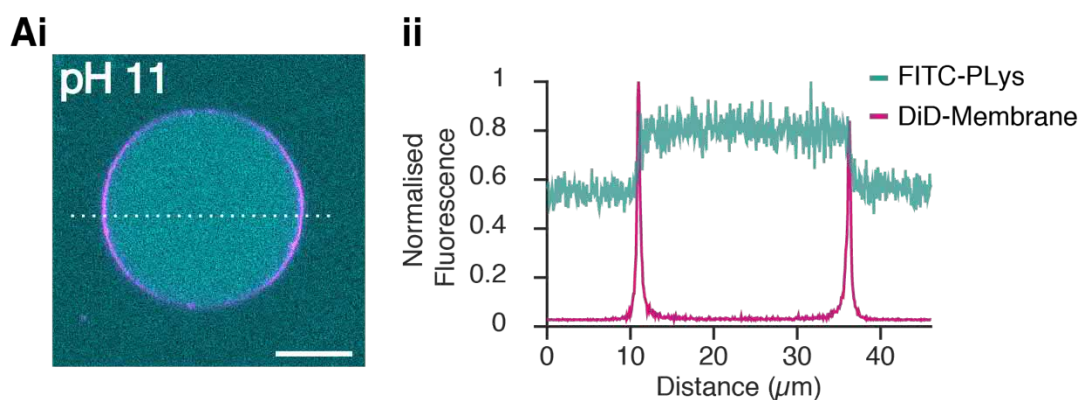


Figure S2. (Ai) Confocal microscopy image showing POPC/cholesterol lipid vesicles doped with DiD dye (0.3% mol) containing PLys and ATP (40/10mM) doped with 0.25 % FITC-PLys at pH 11 after swelling and harvesting of lipid vesicles but before washing. Scale bar 10 μ m. **(ii)** Intensity profile of confocal image (dotted white line) showing fluorescence intensity from FITC-PLys both inside and outside of the lipid vesicle.

SUPPORTING INFORMATION

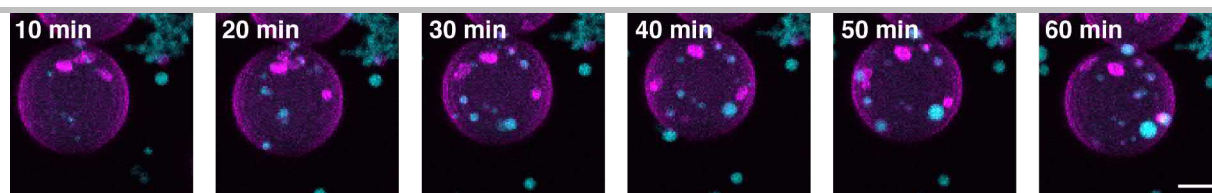


Figure S3. Confocal microscopy max projections of the formation of PLys/ATP coacervates (cyan) in washed GUVs (magenta) over 60 mins after changing the pH from pH 11 to pH 9. The images show the same lipid vesicle. Scale bar 5 μm .

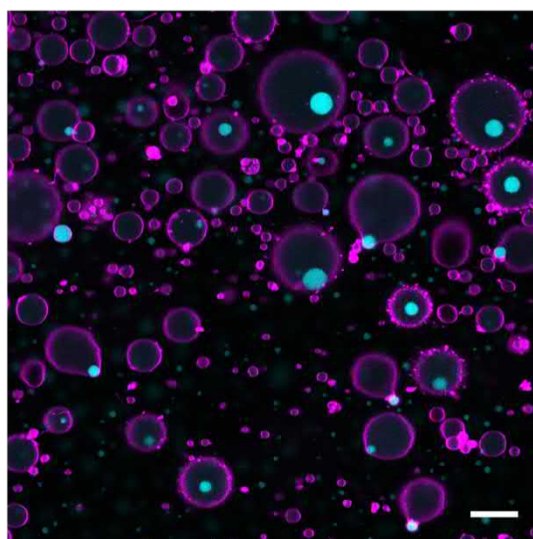


Figure S4. GUVs containing CM-Dextran/PLys coacervates 24 hours after pH switch in the microscopy chamber. Scale bar 10 μm .

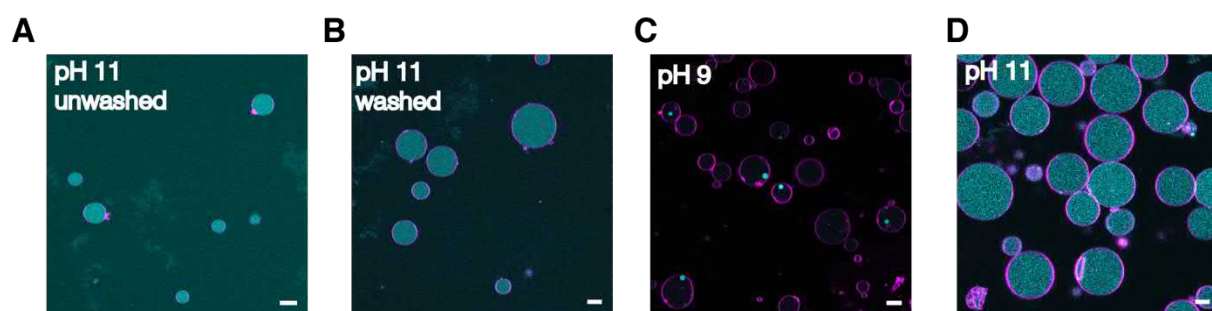


Figure S5. Fluorescent confocal microscopy images showing populations of GUVs fluorescently labelled with DiI dye (0.3 mol %) encapsulating PLys/ATP (40 mM/10mM) doped with 0.25% (v/v) FITC-labelled PLys (A) at pH 11 after swelling, (B) after washing of the lipid vesicles at pH 11, (C) after a pH switch to pH 9 and (D) after returning the pH to pH11. Scale bar 10 μm .

SUPPORTING INFORMATION

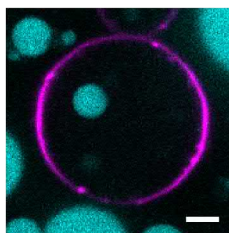


Figure S6. Fluorescent confocal microscopy image showing a GUV fluorescently labelled with DiD dye (0.3 mol %) encapsulating PLys/ATP (40 mM/10mM) as an example for a hybrid cell that underwent the FRAP experiment. Scale bar 5 μm .

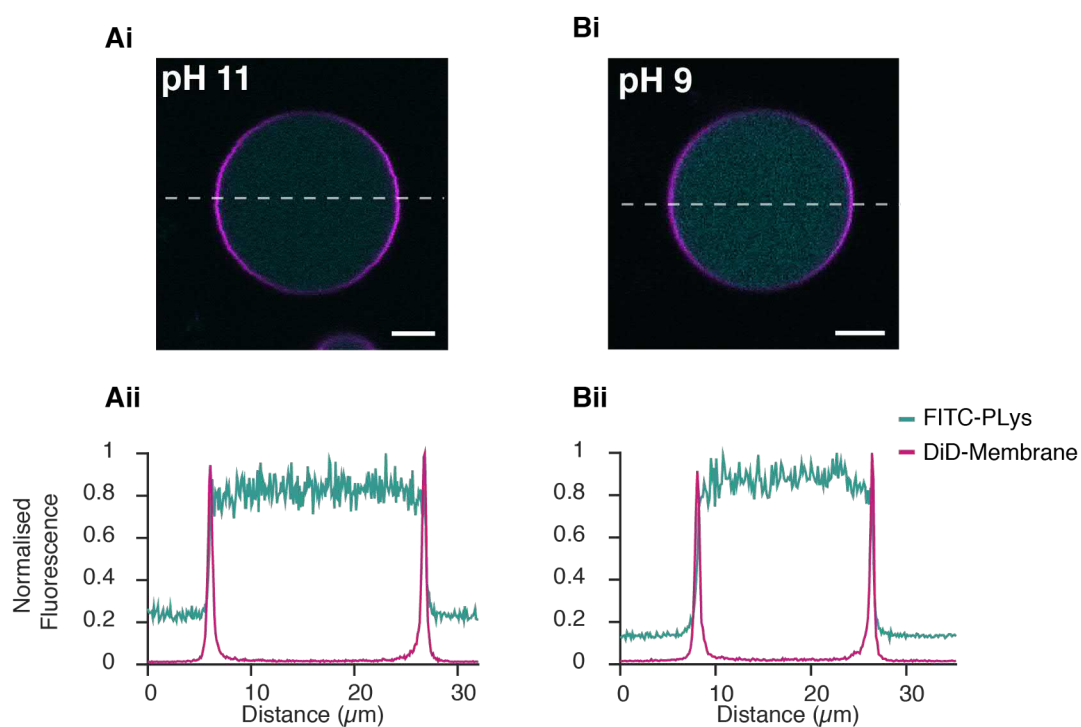


Figure S7. Control experiments of GUVs encapsulating PLys doped with 0.25 % FITC labelled PLys, which have been washed at pH 11 and the pH subsequently reduced to pH 9. Confocal optical microscopy images (i) and corresponding intensity profile across the white dotted line (ii) of **(A)** at pH 11 and **(B)** at pH 9. No coacervates form without ATP within the GUVs after acidification. Scale bar 5 μm .

SUPPORTING INFORMATION

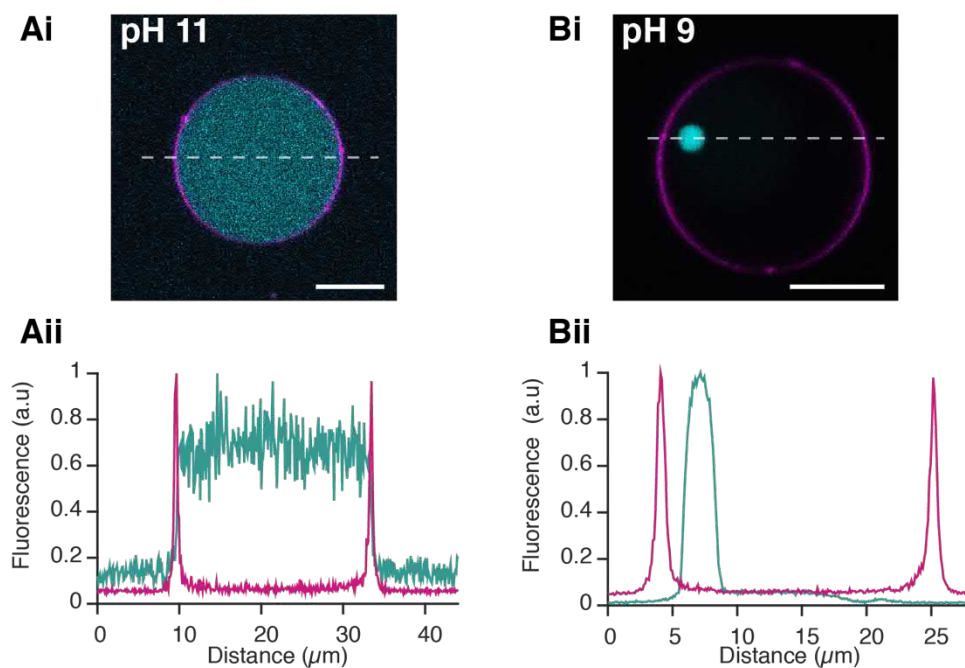


Figure S8. (A) Fluorescent confocal microscopy images showing the up concentration of 0.1 un ml^{-1} of FITC-tagged formate dehydrogenase upon coacervation of CM-Dextran/PLys within a POPC/cholesterol GUV after a pH switch from pH 11 to pH 9 and the corresponding intensity profile **(Aii)**. **(B) (i)** Up-concentration of formate dehydrogenase into the coacervate droplets upon coacervation at pH 9. **(Bii)** Corresponding line profile Scale bar = $5 \text{ }\mu\text{m}$.

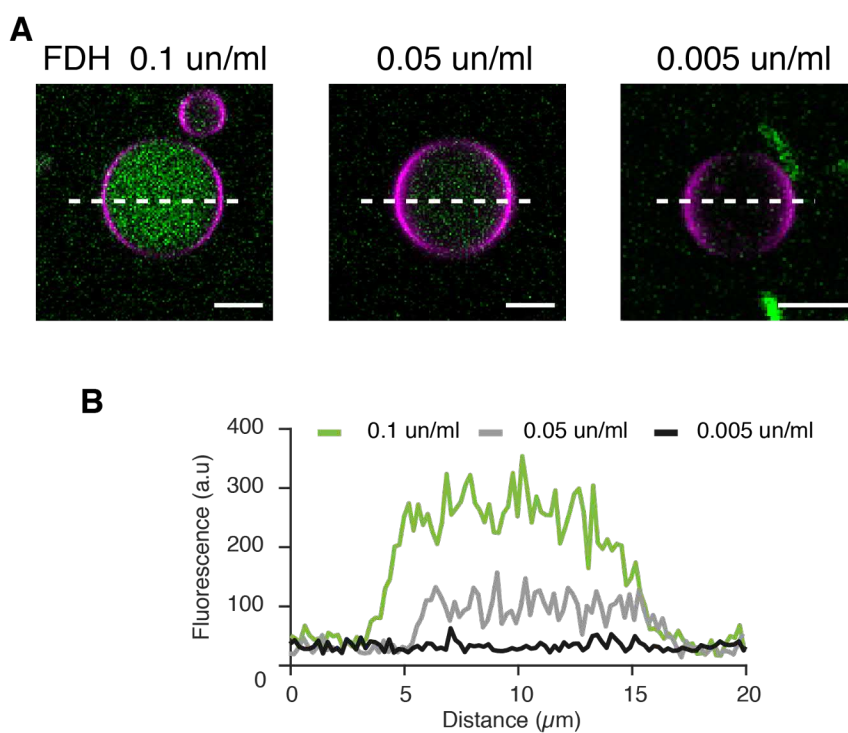


Figure S9. NADH production by formate dehydrogenase within POPC/cholesterol GUVs at pH 9. (A) Fluorescent confocal microscopy images of NADH fluorescence in GUVs encapsulating $\beta\text{-NAD}^+$ (0.45 mM) and formate (5 mM) with decreasing formate dehydrogenase concentration (0.1 , 0.05 , 0.005 un/ml) after 24 hours of incubation at room temperature. Scale bar = $5 \text{ }\mu\text{m}$. **(B)** Intensity plots of NADH fluorescence from GUVs containing 0.1 un/ml (green line), 0.05 un/ml (grey line), 0.005 un/ml (black line). NADH was produced at 0.1 un/ml and 0.05 un/ml but no appreciable NADH fluorescence at 0.005 un/ml . All confocal images were obtained on the same laser intensity and detector gain settings.

SUPPORTING INFORMATION

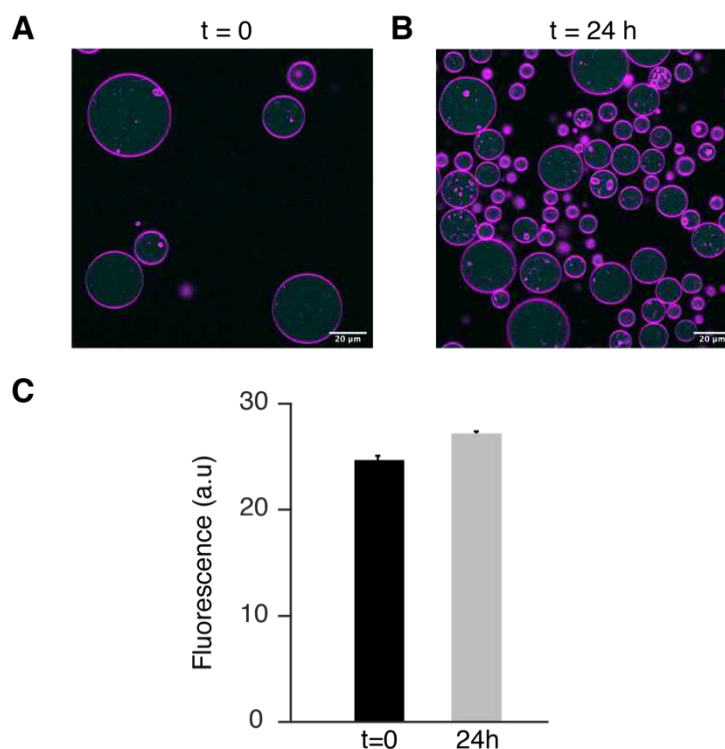


Figure S10. Control experiment showing that FITC tagged formate dehydrogenase remains encapsulated within the vesicles after 24 hrs. (A) Confocal microscopy images of FITC tagged formate dehydrogenase ($0.1 \text{ } \mu\text{M}$) encapsulated within in POPC/cholesterol GUVs at pH 9 at $t = 0$ hrs (B) Images of the same vesicle population after 24 hours. (C) Mean fluorescence intensity of the FITC tagged formate dehydrogenase within the GUVs at $t = 0$ and $t = 24$ hours. The data shows no decrease in fluorescence intensity over 24 hrs. Error bars indicate the standard deviation from at least 20 vesicles.

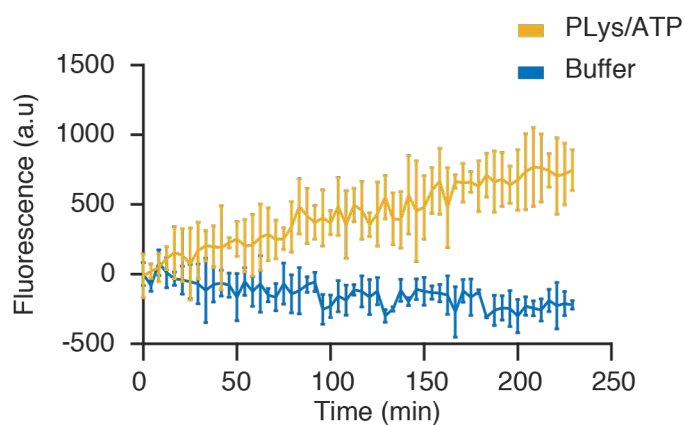


Figure S11. Activity of $0.002 \text{ } \mu\text{M}$ formate dehydrogenase in PLys/ATP (40 mM/ 10 mM) coacervate dispersions in the absence of vesicles obtained using a TECAN Spark 20 M spectrometer. The coacervate and enzyme dispersions were held at pH 11 for 30 mins before reducing to the pH to pH 9. No activity was observed in the buffer. However, formate dehydrogenase was active within the coacervate dispersion and NADH production increased linearly with time.

SUPPORTING INFORMATION

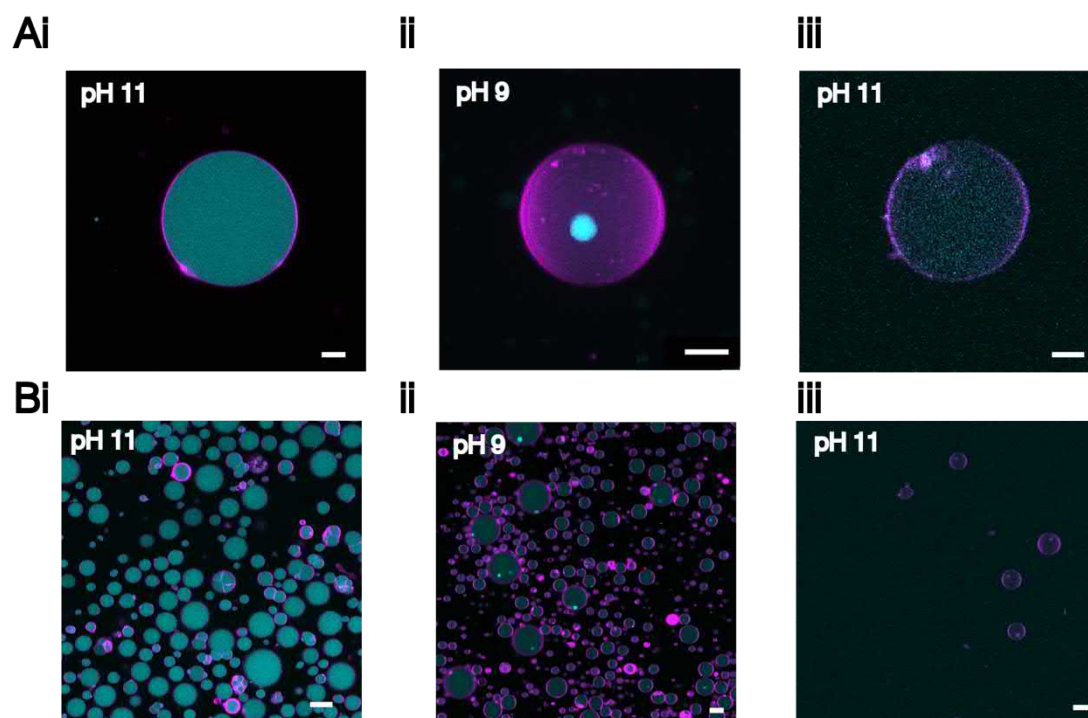


Figure S12. Confocal microscopy images of (A) single POPC/cholesterol GUVs and (B) populations of vesicles containing CM-Dextran/PLys (40 mM/10 mM) (i) at pH 11 where the polymers are diffuse, (ii) at pH 9 where coacervates have formed within the vesicles after a pH switch (note that not all GUVs show the presence of coacervate droplets), (iii) after a return to pH 11, the coacervate droplets dissolve. (A) Scale bar = 5 μm (B) Scale bar = 10 μm .

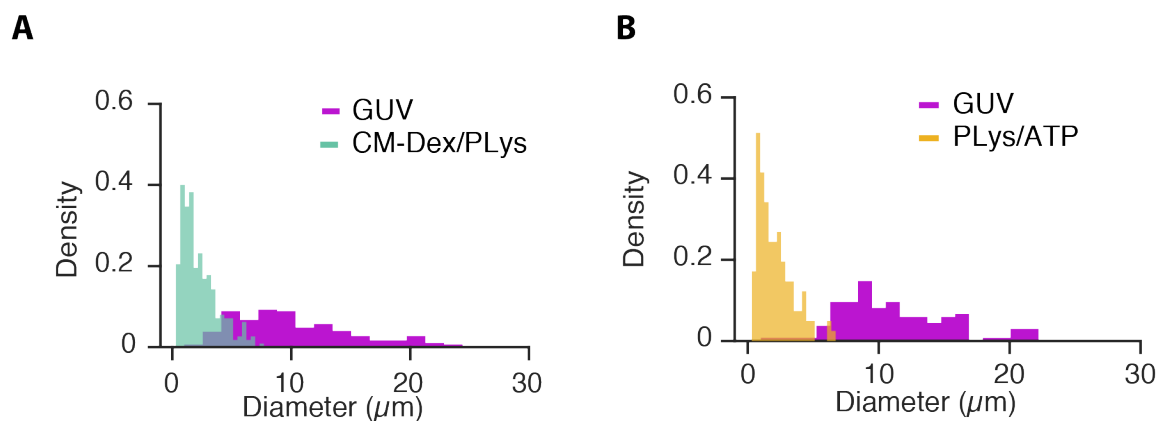


Figure S13 (A) Histogram showing the diameters of the CM-Dextran/PLys coacervates and the corresponding GUVs, $n = 128$. (B) Histogram plotting the diameters of GUVs and PLys/ATP coacervates, $n=304$.

SUPPORTING INFORMATION

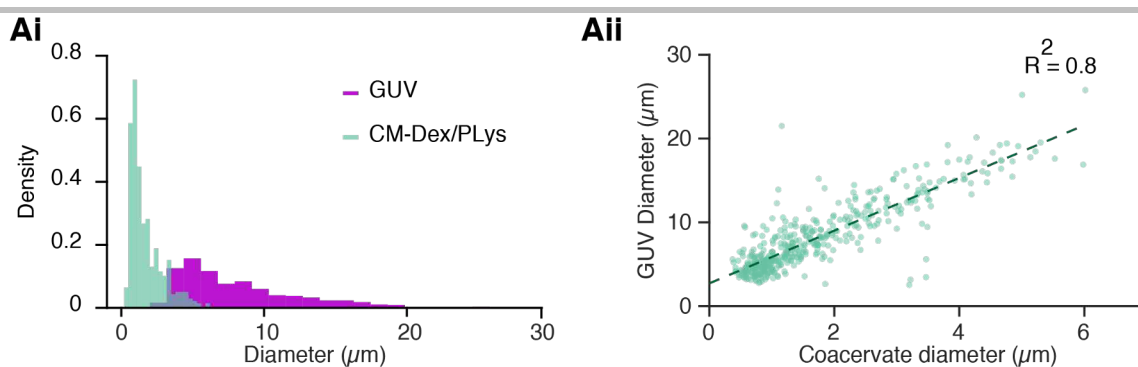


Figure S14. Size characterization of CM-Dextran/PLys coacervates formed in GUVs from a repeat experiment. **(Ai)** Histogram showing the quantified diameters of the CM-Dex/PLys coacervates and their encapsulating GUVs. Mean coacervate diameter $1.70 \pm 1.14 \mu\text{m}$, mean vesicle diameter $8.06 \pm 4.12 \mu\text{m}$, $n > 450$. **(Aii)** Scatter plot of coacervate diameters plotted against vesicle diameters. Data shows a correlation between the size of the GUV that of the encapsulated coacervate. Straight lines fitted to the data gave similar R^2 values of 0.8 compared to other repeat experiments.

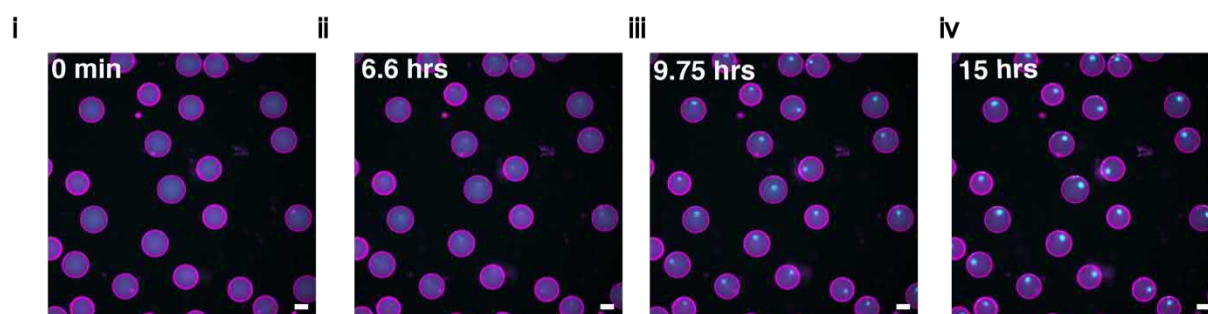


Figure S15. Fluorescent confocal microscopy images of Egg PC lipid vesicles doped with Texas Red DHPE (0.1 mol%) and PLys/ATP coacervates doped with 0.25 % v/v FITC tagged PLys prepared by microfluidic methodologies. The lipid vesicles were prepared at pH 11 and the pH was switched to pH 9. Fluorescence widefield images were obtained at (i) 0 mins, (ii) 6.6 hrs, (iii) 9.75 hrs and (iv) 15 hrs. Scale bar 50 μm .

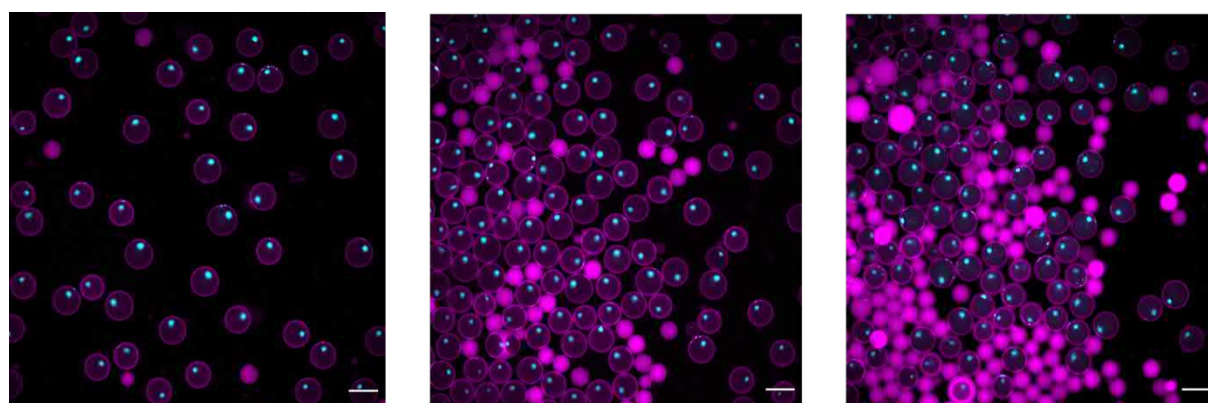


Figure S16. Wide field microscopy images showing three regions of interest of a population of GUVs prepared using microfluidics, 15 hours after a pH switch from pH 11 to 9. Scale bar 100 μm .

References:

- [1] A. Weinberger, F.-C. Tsai, G. H. Koenderink, T. F. Schmidt, R. Itri, W. Meier, T. Schmatko, A. Schröder, C. Marques, *Biophys. J.* **2013**, *105*, 154–64.

SUPPORTING INFORMATION

- [2] R. Eils, C. Kappel, *Confocal Appl. Lett.* **2004**, *18*.
- [3] R. D. Phair, S. A. Gorski, T. Misteli, **2003**, pp. 393–414.
- [4] B. Drobot, J. M. Iglesias-Artola, K. Le Vay, V. Mayr, M. Kar, M. Kreysing, H. Mutschler, T.-Y. D. Tang, *Nat. Commun.* **2018**, *9*, 3643.
- [5] D. Axelrod, D. E. Koppel, J. Schlessinger, E. Elson, W. W. Webb, *Biophys. J.* **1976**, *16*, 1055–1069.
- [6] J. Petit, I. Polenz, J.-C. Baret, S. Herminghaus, O. Bäumchen, *Eur. Phys. J. E* **2016**, *39*, 59.

Author Contributions:

T-Y-D.T. conceived the research and acquired funds. RM and TR contributed funds to the project. CL, JS, DG, RM contributed to the design and the undertaking of the experiments. NY and TR contributed the microfluidic devices. CL analysed the data. CL, JS, CZ, T-Y DT contributed to the interpretation of data. CL, T-YDT wrote the original draft of the manuscript. and all authors contributed to the final manuscript.